

Climate entropy production recorded in a deep Antarctic ice core

Joshua Garland^{1†*}, Tyler R. Jones^{2†}, Elizabeth Bradley^{1,3}, Michael Neuder³, James W. C. White²,

1 Santa Fe Institute, Santa Fe, NM, USA

2 Institute of Arctic and Alpine Research, University of Colorado at Boulder, Boulder, CO, USA

3 Department of Computer Science, University of Colorado at Boulder, Boulder, CO

† These authors contributed equally to this work.

* joshua@santafe.edu

Abstract

Paleoclimate records are extremely rich sources of information about the past history of the Earth system. Information theory, the branch of mathematics capable of quantifying the degree to which the present is informed by the past, provides a new means for studying these records. Here, we demonstrate that estimates of the Shannon entropy rate of the water-isotope data from the West Antarctica Ice Sheet (WAIS) Divide ice core, calculated using weighted permutation entropy (WPE), can bring out valuable new information from this record. We find that WPE correlates with accumulation, reveals possible signatures of geothermal heating at the base of the core, and clearly brings out laboratory and data-processing effects that are difficult to see in the raw data. For example, the signatures of Dansgaard-Oeschger events in the information record are small, suggesting that these abrupt warming events may not represent significant changes in the climate system dynamics. While the potential power of information theory in paleoclimatology problems is significant, the associated methods require careful handling and well-dated, high-resolution data. The WAIS Divide ice core is the first such record that can support this kind of analysis. As more high-resolution records become available, information theory will likely become a common forensic tool in climate science.

Introduction

The Earth contains a vast archive of geochemical information about the past and present states of the climate system. The data in these records—samples from corals, marine and lake sediments, tree rings, cave formations, the ice sheets, etc.—captures a rich spatiotemporal picture of this complex system. Ice cores, for example, provide high-resolution proxies for hydrologic cycle variability, greenhouse gases, temperature, and dust distribution, among other things. While a great deal of sophisticated and creative work has been done on these records, very little of that work has leveraged the power of information theory. The Shannon entropy rate [1, 2], for instance, measures the average rate at which new information—unrelated to anything in the past—is produced by the system that generated a time series. If that rate is very low, the current observation contains a significant amount of information about the past; conversely, if it

is very high, most of the information in the observation is completely new: i.e., the past tells you nothing about the future.

This technique can bring out valuable new information from paleoclimate data records. Here, we use information theory on the longest continuous and highest-resolution water-isotope record yet recovered from Antarctica: the West Antarctica Ice Sheet (WAIS) Divide core. We show that the Shannon entropy rate of these data correlates with accumulation at the ice-core drilling site, reveals possible signatures of geothermal heating at the base of the core, and clearly brings out laboratory and data-processing effects that are difficult to see in the raw data. These information-theoretic calculations not only corroborate known facts and reveal hidden problems with the data, but also suggest new and sometimes surprising geoscience, and pave the way towards more-advanced interhemispheric entropy comparisons that could elucidate some deeper questions about the larger climate system. The signatures of Dansgaard-Oeschger events in the information record are small, for instance, suggesting that these large, abrupt events may not represent significant changes in the climate system dynamics.

To our knowledge, this paper, and the associated pilot study [3], is the first information-theoretic analysis of an ice-core record. Several useful applications of various entropic measures to time-series data about Earth's *current* climate are reviewed in [4], and there is a single published study that used the Shannon entropy rate to explore different climate-change events captured in El Niño/Southern Oscillation proxy records derived from the Laguna Pallcacocha sedimentary data [5]. These kinds of studies are important; for ice core records, knowledge as to where information is created in the climate system, and how it propagates through that system, could help to reveal and elucidate triggers, amplifiers, sources of persistence, and globalizers of climate change [6, 7].

Materials and Methods

Ice Core Data Collection and Description

For the analysis reported here, we used the ratios of $^2\text{H}/^1\text{H}$ and $^{18}\text{O}/^{16}\text{O}$, from the West Antarctic Ice Sheet Divide core (WDC), abbreviated δD and $\delta^{18}\text{O}$, respectively. The record was analyzed using a Picarro Inc. cavity ring-down spectroscopy (CRDS) instrument, coupled to a continuous flow analysis (CFA) system [8]. The data are reported in delta (δ) notation relative to Vienna Standard Mean Ocean Water (VSMOW, $\delta^{18}\text{O} = \delta\text{D} = 0\text{‰}$), normalized to the Standard Light Antarctic Water (SLAP, $\delta^{18}\text{O} = -55.5\text{‰}$, $\delta\text{D} = -428.0\text{‰}$) scale. The δ values were determined by $\delta = 1000(R_{\text{sample}}/R_{\text{VSMOW}} - 1)$, where R is the isotopic ratio $^{18}\text{O}/^{16}\text{O}$ or D/H (i.e., $^2\text{H}/^1\text{H}$). At the WAIS Divide, $\delta^{18}\text{O}$ and δD are proxies for local temperature and regional atmospheric circulation resulting from variability in the hydrologic cycle. Water-isotope data measured on the Picarro instrument were recorded at a rate of 1.18 Hz (0.85 s intervals). Ice samples were moved through the CRDS-CFA system at a rate of 2.5 cm/min, yielding millimeter resolution. The data were then averaged over non-overlapping 0.5 cm bins. For each of these data points, an age was determined using the WDC depth-age scale, providing climate data from 0–68 ka [9]. Annual dating of this record extends to 31 ka [10], with the remainder relying on tie points to the Hulu Cave timescale [11].

Entropy Rate Estimation

The Shannon entropy rate [1] is typically calculated from *categorical* data: sequences of symbols, like heads and tails for a coin-flip experiment. To calculate it from continuum data like δD and $\delta^{18}O$, one must first convert those data into symbols. The typical approach to this—binning—introduces bias and is fragile in the face of noise [12, 13]. The permutation entropy of [14] solves that problem using ordinal analysis, which involves mapping successive elements of that time series to value-ordered permutations of the same size. For example, if successive values of a time series x_i are $(x_1, x_2, x_3) = (6, 1, 4)$ then the ordinal pattern, $\phi(x_1, x_2, x_3)$, of this three-letter “word” is 231 since $x_2 \leq x_3 \leq x_1$. The ordinal pattern of the permutation $(x_1, x_2, x_3) = (60.1, 15.8, 4.0)$ is 321. By calculating statistics on the appearance of these permutations in a sliding window across a signal, one can assess its predictability—that is, how much new information appears at each time step, on the average, in that segment of the time series [15, 16].

Formally, given a time series $\{x_i\}_{i=1, \dots, N}$, there is a set \mathcal{S}_ℓ of all $\ell!$ permutations π of order ℓ . For each $\pi \in \mathcal{S}_\ell$, one defines the relative frequency of that permutation occurring in $\{x_i\}_{i=1, \dots, N}$:

$$p(\pi) = \frac{|\{i | i \leq N - \ell, \phi(x_{i+1}, \dots, x_{i+\ell}) = \pi\}|}{N - \ell + 1} \quad (1)$$

where $p(\pi)$ quantifies the probability of an ordinal and $|\cdot|$ is set cardinality. The permutation entropy of order $\ell \geq 2$ is:

$$PE(\ell) = - \sum_{\pi \in \mathcal{S}_\ell} p(\pi) \log_2 p(\pi) \quad (2)$$

Since $0 \leq PE(\ell) \leq \log_2(\ell!)$ [14], it is common in the literature to normalize by $\log_2(\ell!)$, producing PE values that range from 0 to 1.

Note that permutation entropy, as defined above, does not distinguish between $(x_1, x_2, x_3) = (6, 1, 4)$ and $(x_1, x_2, x_3) = (1000, 1, 4)$ and so it can fail if the observational noise is larger than the trends in the data but smaller than its large-scale features. One can address this issue by introducing a weighting term into the calculation. This variant of the technique—weighted permutation entropy or WPE [17]—is used for all calculations in this paper, again with a normalization that causes the resulting values to run from zero (no new information; fully predictable) to 1 (all new information; completely unpredictable).

To calculate WPE as a function of time, one must have evenly sampled data. This is a major issue here because the 0.5 cm spacing of the samples, combined with the nonlinear age-depth relationship of the core, produce a data series whose temporal spacing increases with depth¹. In order to calculate WPE from these data, we used linear interpolation to achieve uniform 1/20th yr spacing. This is not without issues, as linear interpolation introduces ramps in the signal: repeating patterns in the permutations that can skew their distribution and thereby lower the WPE. Note that this effect will generally worsen with depth because the percentage of interpolated points in the 1/20th-year spaced versions of the δD and $\delta^{18}O$ traces is a nonlinear function of the depth in the core. The specific form of this effect will also depend on the shape of the signal. The mathematics of information theory currently offers no way to approach any kind of closed-form derivation of these complicated effects. In the face of this, it is important to be mindful of interpolation-induced effects in WPE calculations. Among other things, one should not compare WPE values of a single trace from an ice

¹One could certainly calculate WPE on these data, but the timeline of the result would be skewed.

core across wide temporal ranges if the data have undergone depth-dependent interpolation, especially when one is working deep in the core.

Successful use of the WPE method also requires good choices for its three free parameters: the delay τ between samples, the word length ℓ , and the size W of the sliding window over which the statistics are calculated for each WPE value. (In the examples above, $\ell = 3$ and $\tau = 1$.) Very little mathematical guidance is available for these choices and their effects are not independent. The τ parameter controls the spacing of the permutation elements. For low τ values, permutations are strongly affected by high-frequency deviations; for larger τ , those deviations are filtered out. The window size W controls the resolution of the analysis. The word length ℓ must be long enough to allow the discovery of forbidden ordinals, yet small enough that reasonable statistics over the ordinals can be gathered in a window of that size. Choices for the window size and the word length are thus in some tension, since one generally wants the best possible temporal resolution. In the literature, $3 \leq \ell \leq 6$ is a standard choice, generally without any formal justification. In theory, the permutation entropy should converge to the Shannon entropy rate as $\ell \rightarrow \infty$, but that requires an infinitely long time series [18,19]. In practice, the right thing to do is to calculate the *persistent* permutation entropy by increasing ℓ until the large-scale features of the resulting curve converge. That approach was used to choose $\ell = 4$ for the calculations in this study. This value represents a good balance between accurate ordinal statistics and finite-data effects. That ℓ value, in turn, dictated a minimum window size of 2400 points [15] if one considers 100 counts per ordinal as sufficient. This translates to 120 years' worth of ice in the 1/20th-year spaced WDC traces used here.

Results and Discussion

WPE calculations on the δD and $\delta^{18}\text{O}$ data from the WDC, shown in Fig 1, reveal how much new information appears, on average, in a sliding 120-year window leading up to each time point. A number of features stand out here. The WPE values of both isotopes are much lower during the glacial period, for instance, than in the last 5000 years, indicating a stronger dependence of each isotope value on its previous values. During the transition from the glacial to the interglacial, both WPE traces rise sharply at first, beginning around 17 ka, then fall during the Antarctic Cold Reversal (ACR) period before peaking at the time of the transition from the Younger Dryas to the late Holocene, coincident with the time of a known spike in accumulation [20]. This alignment of changes in WPE with known shifts in the climate system suggests that this technique is extracting meaningful information from the paleorecord. As we will show, there are other features in WPE that correlate with known climate information—most strongly, accumulation. There are also distinct *differences* between the two WPE traces, particularly in ice older than 45 ka. Some of these correlations and disparities, we will argue, may be scientifically meaningful.

The τ parameter in the WPE formula, which controls the “stride” of the calculation, plays a role similar to that of the cutoff frequency of a low-pass filter. Fig 2 shows a series of δD and $\delta^{18}\text{O}$ WPE calculations with a range of τ values. Since the τ at which a feature disappears is related to the time scales of the associated effect, one can preferentially focus on—and distinguish between—long-term effects (e.g., climate) or faster ones (e.g., weather) simply by tuning τ . WPE calculations can also reveal the presence of noise in a signal, as is clear from the large bump from 5-8 ka in the black traces in Fig 2. An older instrument was used to analyze the ice in this region; closer examination of the data revealed that, as the WPE results suggested, that instrument introduced significant noise into the data. Note that this instrument noise is not visually apparent in the δD and $\delta^{18}\text{O}$ measurements in Fig 1: that is, WPE is

extracting new information from these data. Increasing τ generally raises the WPE curves; this simply reflects decreasing predictability over the longer time span sampled by each permutation. A feature that persists across a range of τ s, then, such as the set of bumps between $\approx 9 - 14$ ka in Fig 2, indicates an effect in the underlying signal that spans multiple time scales. Broad-band noise manifests somewhat differently: as a jumbled set of WPE curves with no clear trend with τ (cf., in both δD and $\delta^{18}O$ traces below ≈ 60 ka)². All of these patterns—a sharp shift at a particular τ value for a band-limited effect, clear features that persist across a range of τ s for effects that span multiple time scales, and jumbles of curves for broad-band noise or temporal shuffling—are recognizable and diagnostic.

WPE also flags other kinds of problems in the data. The spikes around 58 ka in Figs 1 and 2 offer one compelling example. In this region, 1.107 m (110.1 yr) of ice was missing from the record. Interpolating across this gap with a 1/20th year spacing introduced ≈ 2387 points, in the form of a linear ramp with positive slope: in other words, a long series of “1234” permutations. This causes a drop in WPE as the calculation window passes across this expanse of interpolated, highly predictable values. For calculations with $\tau = 1$ and $W = 2400$, there is a brief period where 99.45% of the “data” in that window has the same permutation, which causes WPE to fall precipitously, then spike back up as the window starts to move back onto non-interpolated data.

²Signals that are temporally shuffled also produce this WPE pattern.

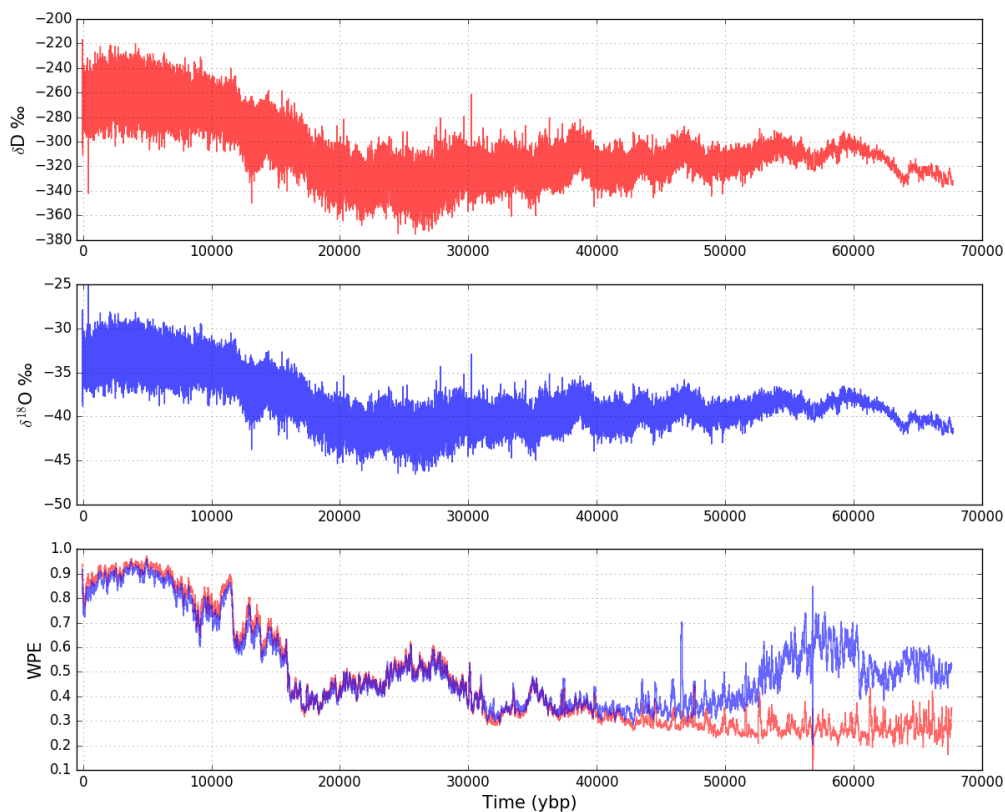


Fig 1. WAIS Divide Core: water isotope values and permutation entropy. The δD and $\delta^{18}O$ data and the weighted permutation entropy (WPE) calculated from those data are shown in color (red for δD and blue for $\delta^{18}O$). The large spikes in both WPE traces near 58 ka are due to a 110-year gap in the isotope record.

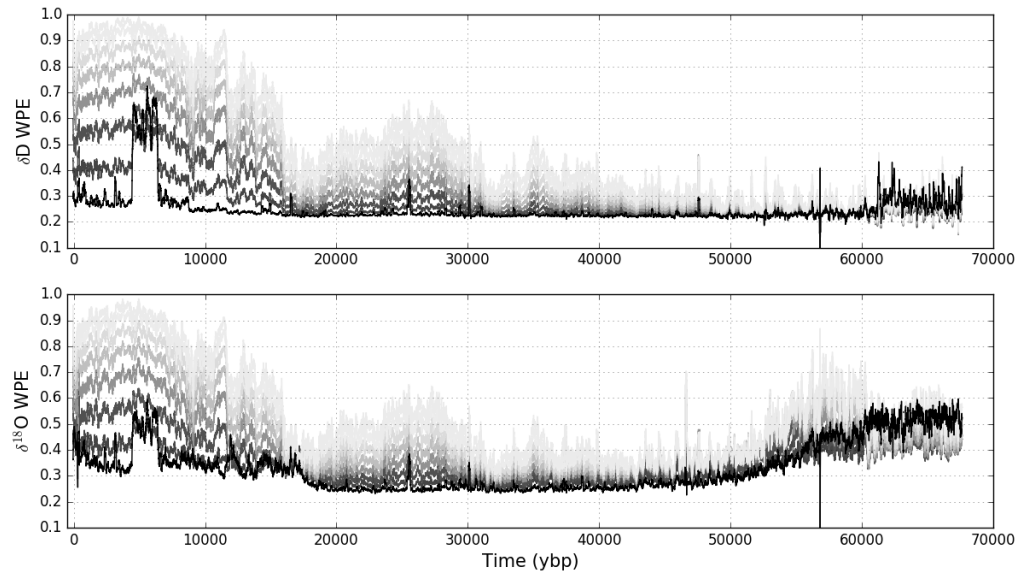


Fig 2. The effects of τ on WPE. δD and $\delta^{18}O$ WPE calculated for different sample spacings $1 < \tau < 8$, with the $\tau = 1$ trace shown in black and larger τ values in successively lighter shades of grey. (Fig 1 uses $\tau = 7$.)

Larger τ values—the grey traces in Fig 2—mitigate this effect because they widen both the spacing and the span of the permutation. Larger window sizes also mitigate this effect (see Fig S1), but they also decrease the temporal resolution of the WPE analysis.

Outliers in the data that are all but invisible in δD and $\delta^{18}O$ traces also leave clear signatures in WPE, in the form of square waves that are the width of the calculation window—e.g., at ≈ 48 ka in the δD trace in Fig 2. (See Fig S2 for an expanded view of this region of the trace, together with the raw δD data in that region.) Upon closer examination, it is clear that the data in that region are problematic. Alerted by a small square wave in WPE, then, one can do a targeted re-analysis of the raw data in the corresponding region.

Another prominent feature in both Figs 1 and 2 is the divergence between the δD and $\delta^{18}O$ WPE traces near the base of the ice sheet. In this part of the record, the signal-to-noise ratios in the data are low, which will raise the WPE. This effect, which is stronger in $\delta^{18}O$ than in δD because the $\delta^{18}O$ values are much smaller, is possibly the cause of the steady rise in the $\delta^{18}O$ WPE trace between ≈ 47 -57 ka. Since the signal-to-noise ratio declines with depth, this rise should, in the absence of any other effects, continue to the end of the WPE trace. However, it does not; rather, $\delta^{18}O$ plateaus at 57-60 ka, then decreases at 60 ka. This suggests that other factors are mitigating the noise effects. There are two likely causes. In this region, the fraction of the points that were produced via interpolation is large, which should, as described in the Materials and Methods section, lower the WPE, and in a manner that increases nonlinearly with depth. Thermal diffusion effects due to geothermal heat at the bedrock interface may also be at work, enhancing diffusion at the base of the ice flow and lowering WPE—and perhaps differentially affecting δD and $\delta^{18}O$ due to their different molecular masses. The δD WPE trace, on the other hand, declines slowly for ages older than 40 ka, indicating a long-term loss in information without a competing noise-induced effect. This makes sense in view of the much higher signal-to-noise ratio of the δD data and suggests that diffusive smoothing may have initiated as early as ≈ 40 ka. This chain of reasoning illustrates that WPE is not merely a way to identify problems with

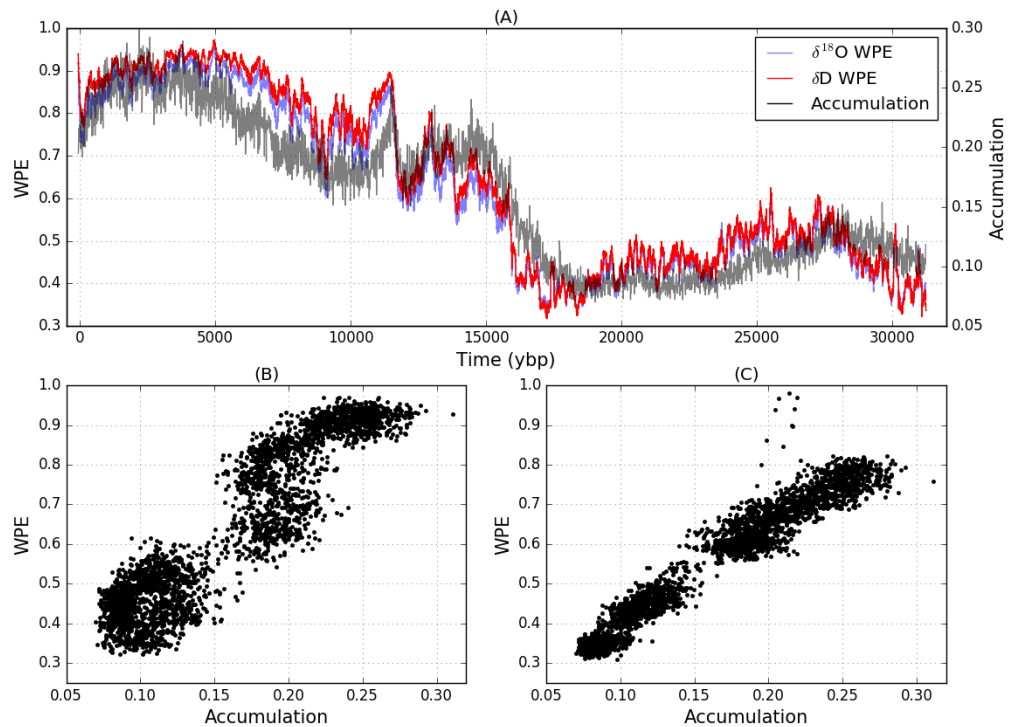


Fig 3. WPE and accumulation. (A) time-series traces of δD WPE (red), $\delta^{18}\text{O}$ WPE (blue), and accumulation (grey) at the WAIS Divide. Bottom: correlation plots of accumulation and δD WPE values from (B) the WDC and (C) a Community Firn Model run [21], respectively. Perfect correlation on the bottom two plots would be a diagonal line. All signals were averaged over non-overlapping 10-year bins to bring out the structure of the plots.

data, but actually a scientific tool that can isolate regions of the paleorecord where interesting findings may be lurking, and even suggest conjectures about those findings.

Another interesting scientific finding brought out by WPE is the relationship between WPE and accumulation, which is explored in Fig 3. Visual examination of part (a) of this figure suggests significant correspondence between the features: many of the bumps, troughs, and trends in the three curves occur at the same times in the record. From first principles, it is not surprising that WPE tracks accumulation. Isotope diffusion intermingles the information in neighboring layers of the core, which will lower the WPE. But there are spatial scales involved in that process, since the diffusion rate depends on the density of the ice. And if the annual layer is thicker, less of the information in that layer will be lost. In other words, accumulation mitigates diffusion effects, thereby preserving the information that was laid down in the core. This means that the low WPE value during the glacial period may not imply that the climate was more predictable then; rather, this may simply be due to lower accumulation. (Diffusion effects may also be the reason why the curves in Fig 2 cluster tightly in some regions—e.g., near 17.5 ka, where there is a sharp spike in the diffusion rate at the WDC [22].)

WPE does not track accumulation perfectly, though; it plateaus earlier in the Holocene, for instance, and contains some structure during the glacial period that is not present in the accumulation trace. The correlation plot in Fig 3(b) explores these relationships in more detail. While the WDC results do show a general trend with

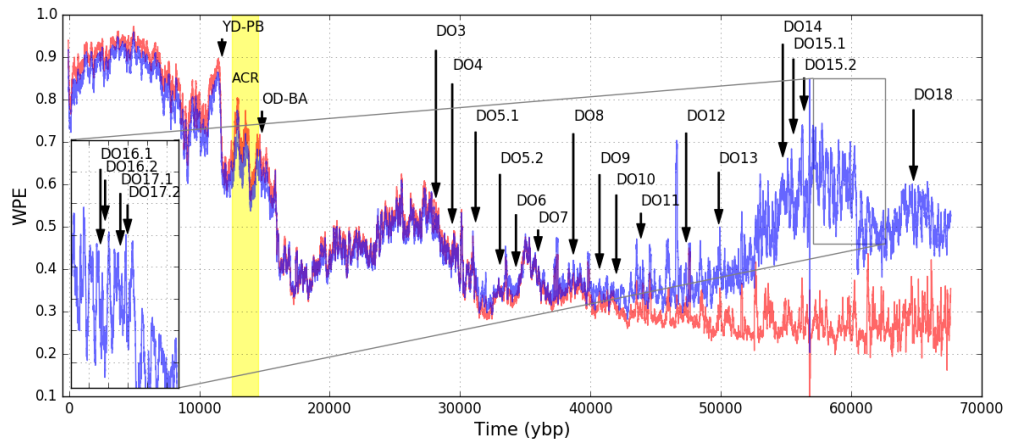


Fig 4. WPE with Dansgaard-Oeschger events labeled for comparison. WPE of δD (red) and $\delta^{18}O$ (blue) with Dansgaard-Oeschger, Antarctic Cold Reversal, and Younger & Older Dryas events shown.

accumulation, it is not entirely linear ($R^2 = 0.927$). We conjecture that these deviations from linearity encode climate signal. To explore this, we obtained a Community Firm Model run [21] with the accumulation rate and temperature set to that measured at the WAIS divide [20] and the water-isotope input fixed throughout the record at a constant annual amplitude and no variation in the mean. See S1 Appendix for the details of this computation. The results show a more-strongly linear relationship ($R^2 = 0.968$) between modeled WPE and accumulation; see Fig 3(c). That is, WPE and accumulation are very tightly correlated in a model run that includes no climate variability. This confirms the underlying linear relationship that is suggested by the climatology, thereby adding weight to the conjecture that the deviations from linearity may be encodings of climate signal.

Another interesting property of the WPE traces is what is *not* there: specifically, there is no systematic correspondence between features in the WDC WPE traces and Antarctic Isotope Maxima (AIM) [23] or Dansgaard-Oeschger (DO) [24] events; see Fig 4. There is a clear peak in WPE at the time of the Younger Dryas event, but that is probably due to the accumulation effects described above. Spectral analysis of the WPE traces (see S1 Table) shows that while millennial frequencies persist throughout the records, they are not 99% statistically significant. That is, we do not see concrete evidence of any persistent frequencies that might correspond to a repeating trigger mechanism of DO and AIM events. Rather, the WPE analysis suggests that while these events substantially changed the climate, they may not have represented substantial changes in the information mechanics of the Earth climate system.

Absence of evidence, of course, is not evidence of absence. This is a particularly thorny point when one is using nonlinear statistics on sparse data. In the literature on WPE, the important issue of significance—whether or not a given feature in a WPE trace (e.g., jump, spike, valley) indicates some sort of substantive change in the underlying information mechanics of the system—is almost never addressed. The basic challenge is that there is no one-to-one correspondence between distributions and entropy values. A very recent paper [25] offers some preliminary solutions to this problem, providing a variant of permutation entropy that measures how far the signal is from white noise and supplies significance bounds. However, this is far from a general solution; with only one time series available, traditional significance tests from statistics are inapplicable. While there are several pseudo significance tests, such as feature

persistence over ranges of parameters, the associated theories are undeveloped. Traditional methods like randomized bootstrapping [26] may eventually be useful here, but the associated mathematics has not yet been extended to information theory in general and WPE in particular. Until these shortcomings have been addressed, interpreting small-scale fluctuations—such as those near the DO events in Fig 4—should either be avoided altogether or done with careful consideration and utilization of domain knowledge and persistence testing over a wide range of values for the free parameters of the algorithm.

Conclusion

The central claim of this paper is that the climate information captured in paleorecords can be better understood with the aid of information theory. As evidence for this claim, and of the traction that it can offer on paleoclimatology problems, we demonstrated that estimates of the Shannon entropy rate of the water-isotope data from the WAIS Divide Core, calculated using weighted permutation entropy (WPE), can bring out valuable new information from this record. We found that WPE correlates with accumulation, reveals possible signatures of geothermal heating at the base of the core, and clearly brings out laboratory and data-processing effects that are difficult to see in the raw data. WPE also contains features that do not correspond to well-known climate phenomena (e.g., DO and AIM events), nor to features in the accumulation record. We suspect that these are encodings of climate signal, but the task of separating out that information from the accumulation/diffusion effects is a real challenge because of the complexity of the mathematics of WPE. While information-theoretic measures are powerful, they require careful handling and high-resolution, well-dated data. Data issues and pre-processing steps that affect the timeline can skew their results, as discussed at length in two recent papers [27, 28]. Moreover, these algorithms have a number of free parameters that must be chosen properly. (This is true of any other data-analysis method, of course, though that is not widely appreciated in many scientific fields.) The WAIS Divide ice core is the first ice-core record that is suitable for these types of analyses. As more high-resolution records become available, and the mathematics is developed, information theory will likely become a common forensic tool in climate science.

Supporting information

S1 Table. Spectral analysis. The 99% significant peaks in the centennial and millennial-scale frequency range (350-4500 years). These results were calculated from the δD WPE trace in Figure 1 using the MTM kspectra package [29] with standard parameter values (three tapers, a resolution of 2, and a red-noise null model) and a sampling interval of 0.05 yr to match the timescale of the data.

epoch	$\tau=1$	$\tau=3$	$\tau=5$	$\tau=7$	$\tau=9$
glacial (20-30 ka)	655	546	546	546	546
transition (10-20 ka)	728	273	728	771	1092, 655
holocene (0-10ka)	1191, 728	364	1008, 596	873	1008, 624

S1 Appendix Community Firn Model. The Community Firn Model (CFM) [21] was used to investigate the effects of firn processes on water isotope WPE. In the CFM,

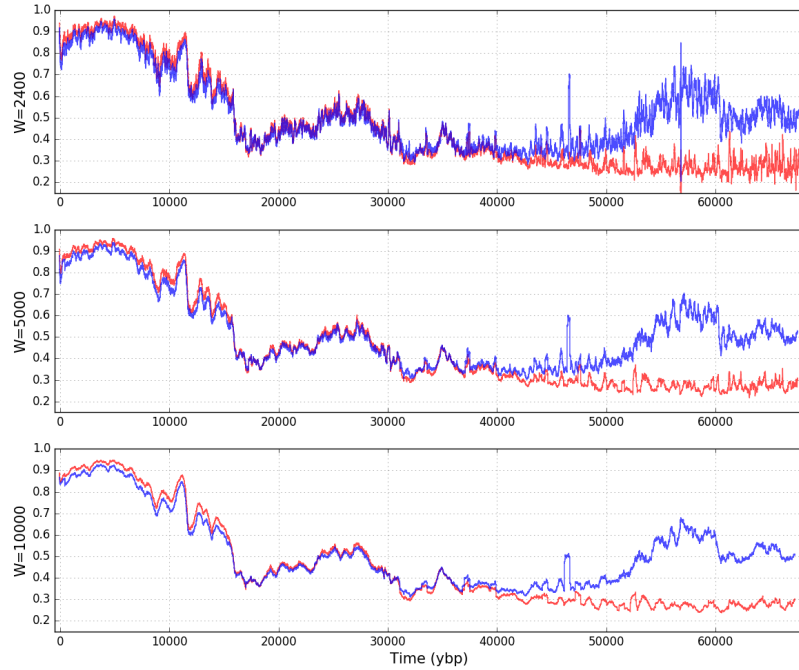


Fig S1. The effect of the window size on WPE. Since WPE aggregates the statistics of the permutations across the calculation window, smaller W values increase the variance and larger W values smooth out the curves—but without changing their overall features. Note that above $W = 2400$, this smoothing removes the 57 ka spikes that were caused by the wide swath of missing isotope data in that region. The bump at ≈ 47 ka is an artifact of a far smaller number of outliers in the $\delta^{18}\text{O}$ data; its changing width reflects the span of the calculation window in which those points play a role. See Fig. S2 for a detailed view of this part of the record.

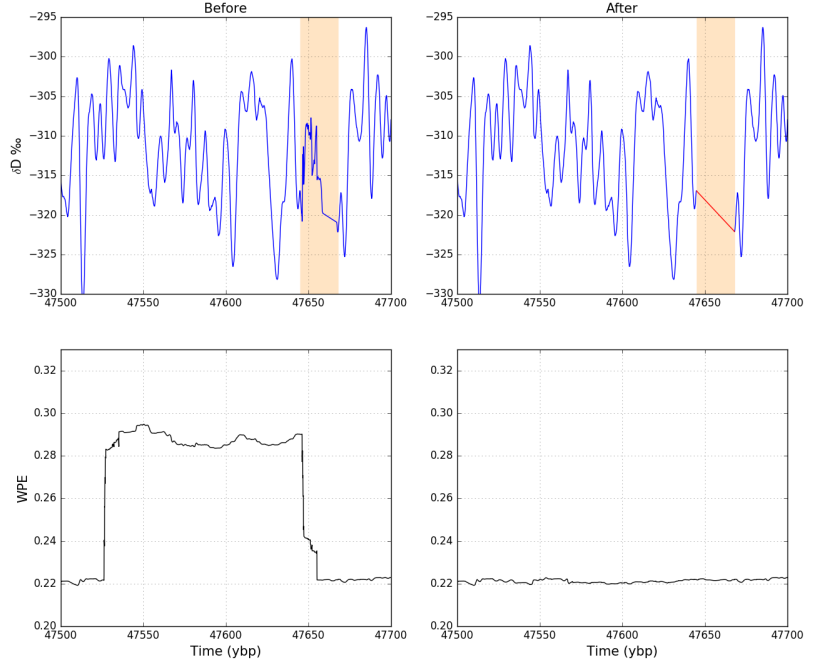


Fig S2. The effects of outliers on WPE. Top row: WDC $\delta^{18}\text{O}$ data from 43–48 ka before and after removal of and interpolation over (red line) a range of faulty values (shaded in tan). Bottom row: WPE calculated from the corresponding traces. As in Fig S1, the width of the square wave in the lower left plot is the size of the WPE calculation window (2400 points at 1/20th year per point). The horizontal shift between the earliest faulty value and the rise in WPE is due to the windowed nature of the WPE calculation.

individual packets of snow/firn/ice are tracked downward over time. At each time step, a new packet is added on top, and the oldest packet is removed from the bottom of the stack. Each packet is compressed at each time step based on its overburden load, temperature, and any other tracked parameters in the model physics. Temperature is also calculated at each step using thermal parameters appropriate for the current density-depth structure.

A synthetic input isotope signal spanning 30 ka was created based on a cosine wave, with an amplitude (a) of 2 ‰, time step (Δt) of 1/12th yr, and a mean value (μ) of -28 ‰:

$$\Delta_{\text{cos}} = a \cos(2\pi t) + \mu$$

Red noise was added to Δ_{cos} to produce the synthetic isotope signal Δ_{syn} for the CFM run:

$$\Delta_{\text{syn}}(i+1) = k\Delta_{\text{cos}}(i) + w(i);$$

where $k = 0.7$ and w is white noise with a standard deviation of 20% of the annual amplitude of the cosine wave. As observed at WAIS Divide, the model depth in the ice sheet at 30 kyr was set to 2816.435 m, and the model depth at the base of the ice sheet was set to 3405 m.

We analyzed two different CFM scenarios, all using the Δ_{syn} signal described above:

1. firn density of 400 kg/m³, estimated temperature at WAIS Divide [30], thermal diffusion ON, estimated accumulation at WAIS Divide [20], and isotope diffusion OFF

2. firn density of 400 kg/m^3 , estimated temperature at WAIS Divide [30], thermal diffusion ON, estimated accumulation at WAIS Divide [20], and isotope diffusion ON

The output for these experiments can be seen in the top two panels of Fig. S3. The second iteration of the CFM model run (shown in grey in Fig. S3) is used in Fig 3. The bottom panel of Fig. S3 reiterates the strong correlation that is described in the Results section between accumulation and WPE when isotopic diffusion is present and the complete lack of correlation when isotopic diffusion is not present.

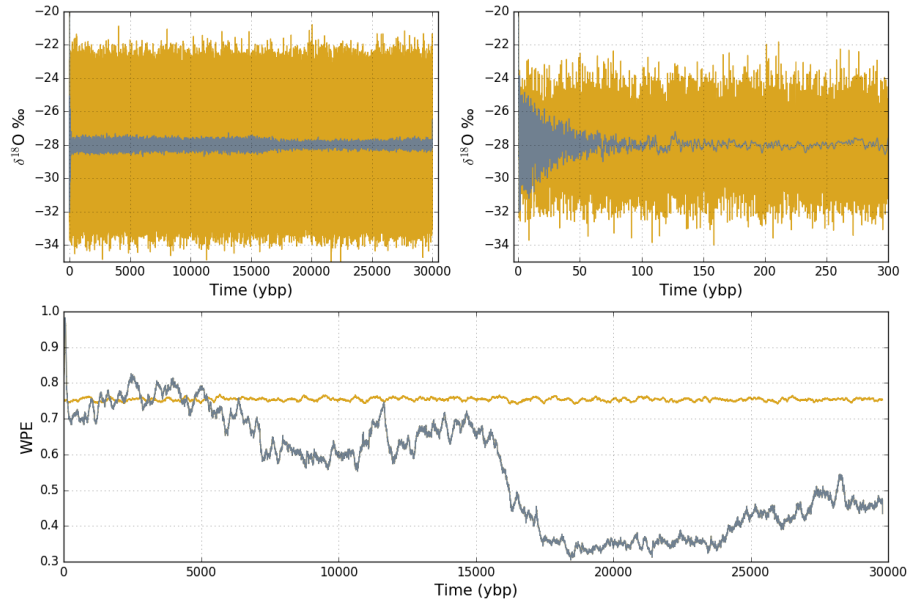


Fig S3. Community Firn Model Results. (a) Synthetic isotope output data for Community Firn Model (CFM) experiment 1 (gold) and experiment 2 (grey) (see Methods). The amplitude of the data in experiment 2 is reduced due to the inclusion of isotopic diffusion in the firn. (b) As in (a), for the most recent 300 years of data. The grey line shows the effects of firn diffusion, which increasingly reduces the signal amplitude until the bubble close-off depth. (c) WPE of CFM output data for experiment 1 (gold) and experiment 2 (grey). The WPE in experiment 2 is very similar to the WDC accumulation rate, due to the combined effects of accumulation and isotopic diffusion in the CFM. See S1 Appendix for more details about these simulations.

References

1. Shannon C. A mathematical theory of communication. *Bell System Technical Journal*. 1948;27(3):379–423.
2. Cover TM, Thomas JA. *Elements of Information Theory*. New York, NY, USA: Wiley-Interscience; 1991.
3. Garland J, Jones TR, Bradley E, James RG, White JWC. A First Step Toward Quantifying the Climate’s Information Production over the Last 68,000 Years. In: Boström H, Knobbe A, Soares C, Papapetrou P, editors. *Advances in Intelligent Data Analysis XV*. Springer International Publishing; 2016. p. 343–355.
4. Balasis G, Donner RV, Potirakis SM, Runge J, Papadimitriou C, Daglis IA, et al. Statistical mechanics and information-theoretic perspectives on complexity in the Earth system. *Entropy*. 2013;15(11):4844–4888.
5. Saco PM, Carpi LC, Figliola A, Serrano E, Rosso OA. Entropy analysis of the dynamics of El Niño/Southern Oscillation during the Holocene. *Physica A: Statistical Mechanics and its Applications*. 2010;389(21):5022–5027. doi:10.1016/j.physa.2010.07.006.
6. Alley R, et al . Abrupt climate change. *Science*. 2003;299:2005–2010.
7. White J, et al . Abrupt impacts of climate change: Anticipating surprises. In: *EGU General Assembly Conference Abstracts*. vol. 16; 2014. p. 17028.
8. Jones TR, White JW, Steig EJ, Vaughn BH, Morris V, Gkinis V, et al. Improved methodologies for continuous-flow analysis of stable water isotopes in ice cores. *Atmospheric Measurement Techniques*. 2017;10(2):617.
9. Jones TR, Roberts WH, Steig EJ, Cuffey K, Markle B, White J. Southern Hemisphere climate variability forced by Northern Hemisphere ice-sheet topography. *Nature*. 2018;.
10. Sigl M, Fudge TJ, Winstrup M, Cole-Dai J, Ferris D, McConnell JR, et al. The WAIS Divide deep ice core WD2014 chronology – Part 2: Annual-layer counting (0–31 ka BP). *Climate of the Past*. 2016;12(3):769–786. doi:10.5194/cp-12-769-2016.
11. Buizert C, Cuffey K, Severinghaus J, Baggenstos D, Fudge T, Steig E, et al. The WAIS Divide deep ice core WD2014 chronology—Part 1: Methane synchronization (68–31 ka BP) and the gas age–ice age difference. *Climate of the Past*. 2015;11(2):153–173. doi:10.5194/cp-11-153-2015.
12. Bollt E, Stanford T, Lai YC, Życzkowski K. What symbolic dynamics do we get with a misplaced partition?: On the validity of threshold crossings analysis of chaotic time-series. *Physica D: Nonlinear Phenomena*. 2001;154(3):259–286.
13. Kraskov A, Stögbauer H, Grassberger P. Estimating mutual information. *Physical Review E*. 2004;69(6):066138.
14. Bandt C, Pompe B. Permutation entropy: A natural complexity measure for time series. *Physical Review Letters*. 2002;88(17):174102.
15. Garland J, James RG, Bradley E. Model-free quantification of time-series predictability. *Physical Review E*. 2014;90(5):052910.

16. Pennekamp F, Iles A, Garland J, Brennan G, Brose U, Gaedke U, et al. The intrinsic predictability of ecological time series and its potential to guide forecasting. Preprint available at bioRxiv 350017. 2018;.
17. Fadlallah B, Chen B, Keil A, Príncipe J. Weighted-permutation entropy: A complexity measure for time series incorporating amplitude information. *Physical Review E*. 2013;87(2):022911.
18. Amigó J. Permutation complexity in dynamical systems: Ordinal patterns, permutation entropy and all that. Springer; 2012.
19. Amigó JM, Kennel MB, Kocarev L. The permutation entropy rate equals the metric entropy rate for ergodic information sources and ergodic dynamical systems. *Physica D: Nonlinear Phenomena*. 2005;210(1-2):77–95.
20. Fudge T, Markle B, Cuffey K, Buizert C, Taylor K, Steig E, et al. Variable relationship between accumulation and temperature in West Antarctica for the past 31,000 years. *Geophysical Research Letters*. 2016;43(8):3795–3803. doi:10.1002/2016GL068356.
21. Lundin JMD, Stevens C, Arthern R, Buizert C, Orsi A, Ligtenberg SRM, et al. Firn Model Intercomparison Experiment (FirnMICE). *Journal of Glaciology*. 2017;63(239):401–422. doi:10.1017/jog.2016.114.
22. Jones TR, Cuffey KM, White JWC, Steig EJ, Buizert C, Markle BR, et al. Water isotope diffusion in the WAIS Divide ice core during the Holocene and last glacial. *Journal of Geophysical Research: Earth Surface*. 2017;122(1):290–309. doi:10.1002/2016JF003938.
23. WAIS Divide Project Members. Precise inter-polar phasing of abrupt climate change during the last ice age. *Nature*. 2015;520:661–665.
24. Dansgaard W, Johnsen SJ, Clausen HB, Dahl-Jensen D, Gundestrup NS, Hammer CU, et al. Evidence for general instability of past climate from a 250-kyr ice-core record. *Nature*. 1993;364(6434):218–220.
25. Bandt C. A new kind of permutation entropy used to classify sleep stages from invisible EEG microstructure. *Entropy*. 2017;19(5). doi:10.3390/e19050197.
26. Efron B, Tibshirani R. Bootstrap Methods for Standard Errors, Confidence Intervals, and Other Measures of Statistical Accuracy. *Statistical Science*. 1986;1(1):54–75.
27. McCullough M, Sakellariou K, Stemler T, Small M. Counting forbidden patterns in irregularly sampled time series. I. The effects of under-sampling, random depletion, and timing jitter. *Chaos: An Interdisciplinary Journal of Nonlinear Science*. 2016;26(12):123103.
28. Sakellariou K, McCullough M, Stemler T, Small M. Counting forbidden patterns in irregularly sampled time series. II. Reliability in the presence of highly irregular sampling. *Chaos: An Interdisciplinary Journal of Nonlinear Science*. 2016;26(12):123104.
29. Ghil M, Allen MR, Dettinger MD, Ide K, Kondrashov D, Mann ME, et al. Advanced Spectral Methods for Climatic Time Series. *Reviews of Geophysics*. 2002;40(1):3–1—3–41. doi:10.1029/2000RG000092.

30. Cuffey KM, Clow GD, Steig EJ, Buizert C, Fudge TJ, Koutnik M, et al. Deglacial temperature history of West Antarctica. *Proceedings of the National Academy of Sciences*. 2016;113(50).